

7

A Multi-Scale Analysis of Algerian Oil Borehole Logs Using the Empirical Mode Decomposition

7

A Multi-Scale Analysis of Algerian Oil Borehole Logs Using the Empirical Mode Decomposition

Said Gaci

Sonatrach, Division Exploration, Boumerdès, Algeria. Email: said_gaci@yahoo.com

Summary

This paper presents a multi-scale analysis of well logs recorded in four Algerian oil exploration boreholes, using a scale-based decomposition method, namely Empirical Mode Decomposition (EMD). The main strength of the latter, compared with the traditional approaches, lies in its adaptiveness to study nonlinear and non-stationary data.

Here, the well log data are decomposed into Intrinsic Mode Functions (IMFs) which are investigated considering the lithological subintervals which compose the studied depth interval. For each subinterval, the mean wavenumber (k_m) of each IMF mode (m) indicates that the EMD method acts as an almost a dyadic filter bank. Moreover, the complexity degree of each lithological unit can be measured by the slope (ρ) of the linear fit of the plot k_m vs. m in the log-linear plan. The results show that for a given well, the lithological subintervals are characterized by distinct ρ values. However, the average ρ values estimated for each lithology are very close. Thus, a ρ value can not characterize a given lithology.

7.1 Introduction

In oil and gas exploration, well logs are detailed records of rock and fluid properties of the geological formations crossed by a borehole. The measurements include electrical properties (resistivity and conductivity at various frequencies), acoustic properties, radioactive, electromagnetic, nuclear magnetic resonance, and other properties of the rocks and their contained fluids. An interpretation of these measurements allows to locate and quantify possible depth intervals containing hydrocarbons.

Traditionally, well log data are analyzed using decomposition techniques, such as Fourier decomposition or wavelet decomposition using basis functions. However, the main shortcoming of these tools is originated from the fact that the basis functions are fixed and do not necessarily match the varying nature (non-stationarity and nonlinearity) of those signals.

The Fourier-based analysis does not lead to significant interpretation unless the signal to be analyzed is linear and stationary. As regards the wavelet transform, it is a time-frequency analysis method which gives best results, whereas it fails to get fine resolutions in both time domain and frequency domain simultaneously due to the limitation of Heisenberg-Gabor inequality.

Due to nonlinearity and non-stationarity nature of well logs, their analysis requires data-driven methods, without a priori assumptions basis, i.e. analytical methods using adaptive bases that are derived from the data and appropriate to describe their multi-scale behavior. For this purpose, such a method has been suggested to analyze nonlinear and non-stationary borehole measurements: Empirical Mode Decomposition (EMD).

This adaptive time-frequency data analysis method has been proposed by

Huang et al. (1998, 1999). It gained an increasing attention in a broad range of applications (Gloersen and Huang, 2003; Chiew et al., 2004; Huang and Wu., 2008; Bekara and Van der Baan, 2009; Han and Van der Baan, 2011 ; De Michelis et al., 2012).

The EMD technique consists of decomposing the signal into a sum of oscillatory functions, namely Intrinsic Mode Functions (IMFs), displaying different mean frequencies (or wavenumbers). The investigation of complexity nature of the well logs can be performed by analyzing the number of scales associated with the phenomenon described by the signal, as well as the relationship between the IMFs index and the mean wavenumber.

This rest of this paper is structured as follows: Firstly, we give a brief mathematical description of the EMD algorithm. In section 2, the physical properties measured by the well logs explored in our application are presented, followed by a lithological description of the logged interval in the considered boreholes. The analysis and discussion of the obtained results are presented in Section 3. Finally, the main findings and the perspectives of our research are given in Section 4.

7.2 EMD Algorithm

The EMD algorithm is the main part of the Hilbert-Huang Transform. It provides an efficient tool to decompose a nonlinear and non-stationary signal into a sum of Intrinsic Mode Functions (IMFs) (or modes) without a priori basis as required by traditional Fourier and wavelet-based methods (Huang et al. 1998; 1999; Flandrin et Gonçalvès, 2004).

Each IMF have a characteristic frequency (Wu and Huang, 2004; Flandrin et al. 2004), and must satisfy two simple conditions:

1) The difference between the number of local extrema and the number of zero-crossings must be zero or at most one.

2) At any time point, the mean value of two envelopes estimated by the local maxima and local minima is zero.

The decomposition process, called also a shifting process, is an iterative procedure which can be summarized as follows:

Step 1: Identify all local extrema (maxima and minima) of the signal $X(z)$.

Step 2: Generate the upper $U(z)$ and lower $L(z)$ envelope of the signal connecting, respectively, the local maxima and minima by cubic spline interpolation.

Step 3: Estimate the local mean envelope $m(z)$ of the signal:

$$m(z) = \frac{U(z) + L(z)}{2}$$

Step 4: Extract the local mean $m(z)$ from the signal: $h_1(z) = X(z) - m(z)$.

Step 5: Replace the signal $X(z)$ by $h_1(z)$, and reiterate Steps 1-4 until the resulting signal satisfies the two IMF conditions.

The above shifting process should be stopped by any of the following criteria: after extracting n IMFs, the residue, $r_n(z)$ is either an IMF or a monotonic function. More details on the EMD algorithm and stopping criteria can be found in the literature (Huang et al. 1998, 1999, 2003, 2008; Huang, 2005; Flandrin and Gonçalves, 2004; Rilling et al., 2003; Rilling and Flandrin, 2008).

After completion of EMD the signal can be written as follows:

$$X(z) = \sum_{m=1}^n \text{IMF}_m(z) + r_n(z) \quad (1)$$

where n is the total number of the IMF components .i.e. it is decomposed into n IMFs with one residual.

As it can be noted, the characteristic scale is increasing with the mode index m . Each mode is characterized by a different mean wavenumber estimated by the following relation:

$$k_m = \frac{\int_0^{\infty} k S_m(k) dk}{\int_0^{\infty} S_m(k) dk} \quad (2)$$

where $S_m(k)$ is the Fourier spectrum of m^{th} IMF mode (IMF $_m$). It represents an energy weighted mean wavenumber in the Fourier power spectrum (Huang et al., 1998).

The mode number m of the IMF and the mean wavenumber are related by an exponential law:

$$k_m = k_0 \rho^{-m} \quad (3)$$

where k_0 is a constant and ρ is the slope of the linear fit in the log-linear plot. That means that k_m of IMF $_m$ is approximately ρ times of the next one (IMF $_{m+1}$). This relation indicates that EMD behaves as an adaptive dyadic filter bank of constant-bandpass filters when applied to fractional Gaussian noise (fGn) (Flandrin and Goncalvès, 2004; Flandrin et al., 2004), and white noise (which is a special case of fGn) (Wu and Huang, 2004). For such stochastic noises, the ρ value is very close to 2, as is the case of turbulence time series (Huang et al., 2008). This

parameter measures the multi-scale features and the complexity degree of the signal. When its value decreases, more scales are involved in the description of the phenomenon.

On the other hand, it is demonstrated that for white noise (Flandrin et al., 2004; Wu and Huang, 2004), the EMD acts as a dyadic filter bank and the power spectra of all IMFs collapse to a single shape along the axis of logarithm of period or frequency. Therefore, the expected number of all IMFs is close to $\log_2(N)$ where N is the length of the considered time series. However, in the case of non-white noise data, the total number of IMFs could be smaller than $\log_2(N)$ since some scales might be ignored. This may be also explained by the mode mixing in some scales originated from the intermittent behavior of the signal.

In this study, the EMD algorithm is implemented to decompose log measurements recorded in four Algerian exploration boreholes drilled in different geological settings. The aim is to analyze heterogeneities characterizing lithological units crossed by the wells.

7.3 Well Log Measurements

Boreholes can provide geological information by measuring the geophysical properties of the penetrated formation using wire line logs. Many different parameters of the rocks can be measured and interpreted in term of lithological porosity and of quantity and type of fluids within the pores. The logs studied in this work are: P and S-wave velocities (V_p and V_s), bulk density (ρ_{b}), neutron porosity (n_{phi}), Gamma ray (GR), electrical resistivity (LLD, AT20 and AT90), photoelectric absorption factor (PEF) and natural gamma ray spectroscopy (Th, U and K).

7.4 Geological Setting

The log data under study are recorded in four (04) Algerian boreholes (W1, W2, W3 and W4), drilled, for the needs of the oil/gas exploration, in different locations in Algeria: southwestern (W1 and W2), south-central (W3) and south-eastern (W4).

As regards well W1, the considered depth interval (905.256-1340m) corresponds to the lower Devonian reservoir. From a lithological point of view, this interval is described as follows:

- Layer L1 (905-1130m): alternation of SANDSTONE and SHALE, with some LIMESTONE layers.
- Layer L2 (1130-1340m): SANDSTONE, passing sometimes into SILTSTONE and LIMESTONE.

Regarding well (W2), the investigated depth interval (1149.096-1386.84m) corresponding to the lowest Devonian reservoir. Lithologically, this interval presents an alternation of LIMESTONE, and SANDSTONE, with SHALE.

For well W3, the analyzed depth range (2579.0652-2716.2252m) corresponds to the Triassic reservoir. It is composed of the alternation of SANDSTONE, and SHALE.

The investigated log data of Well W4 are recorded between the depths of 3496.6656m and 4800.7524m. This depth interval corresponds to the Lias reservoir. It is mainly marked by SHALE, and by the presence of fine layers of SANDSTONE.

7.5 Results and Discussion

This section is devoted to analyze the results obtained using the EMD method from the log data recorded in the considered boreholes (Table 1). The measurements corresponding to wells W1, W2, W3 and W4, are presented, respectively, in Figures 1, 2, 3 and 4. All the used logs are recorded with a sampling rate of 0.1524m.

For the needs of our analysis, the studied depth intervals are divided into main lithological units:

- Well W1 (905.256-1130.046 m: alternation sandstone /shale, and 1130.046-1340m: sandstone).
- Well W2 (1149.096-1257.4524 m: sandstone, and 1257.4524-1386.84 m: shale).
- Well W3 (2579.0652- 2655.1128m: sandstone, and 2655.1128-2716.225m: shale).
- Well W4 (3496.6656-4800.7524m: shale).

As detailed in section 2, the EMD method is applied to logs recorded in the considered boreholes in order to decompose them into their corresponding IMFs. For each log, the power spectra of all the obtained IMFs are computed for the lithological subintervals into which the entire logged depth interval has been divided, and the mean wavenumber (k_m) is estimated for each subinterval. Afterwards, the relation (3) is used to evaluate the ρ value, which represents slope of the graph k_m versus index m in the log-linear plan.

Table 1. Physical properties recorded in the considered wells (W1, W2, W3 and W4).

| Physical property | Symbol/ Unit | Well W1 | Well W2 | Well W3 | Well W4 |
|--------------------------------------|---------------------------|---------|---------|---------|---------|
| P-wave seismic velocity | Vp (m/s) | x | x | | x |
| S-wave seismic velocity | Vs (m/s) | | x | | x |
| Bulk density | rhob (g/cm ³) | x | | x | |
| Neutron porosity | nphi (%) | x | | | |
| Gamma Ray | GR (API) | x | x | x | x |
| Photoelectric absorption factor | PEF | x | | x | |
| deep dual laterolog | LLD (Ohm.m) | x | | | |
| Array Induction Two Foot Resistivity | AT20 (Ohm.m) | | x | | x |
| Array Induction Two Foot Resistivity | AT90 (Ohm.m) | | x | | x |
| Thorium gamma ray spectroscopy | Th (ppm) | x | | x | |
| Uranium gamma ray spectroscopy | U(ppm) | x | | | |
| Potassium gamma ray spectroscopy | K(%) | | | x | |

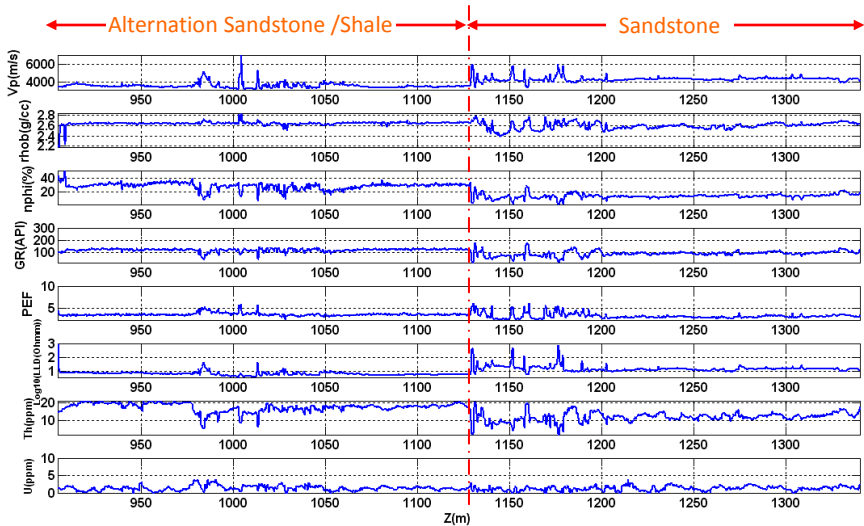


Figure 1. Physical logs measured within the depth interval (905 - 1340m) in borehole W1. Log: decimal logarithm.

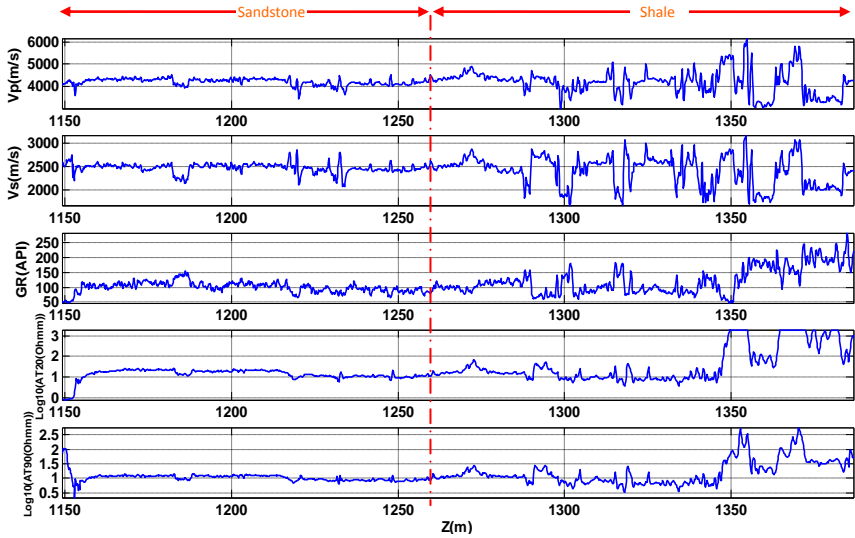


Figure 2. Physical properties measured within the depth interval (1149 - 1387m) in borehole W2. Symbols as in Table 1. Log: decimal logarithm.

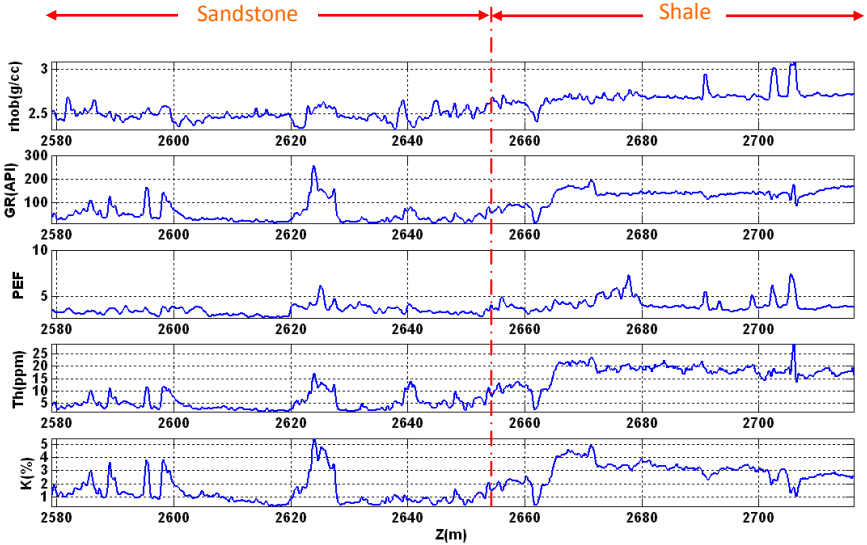


Figure 3. Physical properties measured within the depth interval (2579 - 2716m) in borehole W3. Symbols as in Table 1.

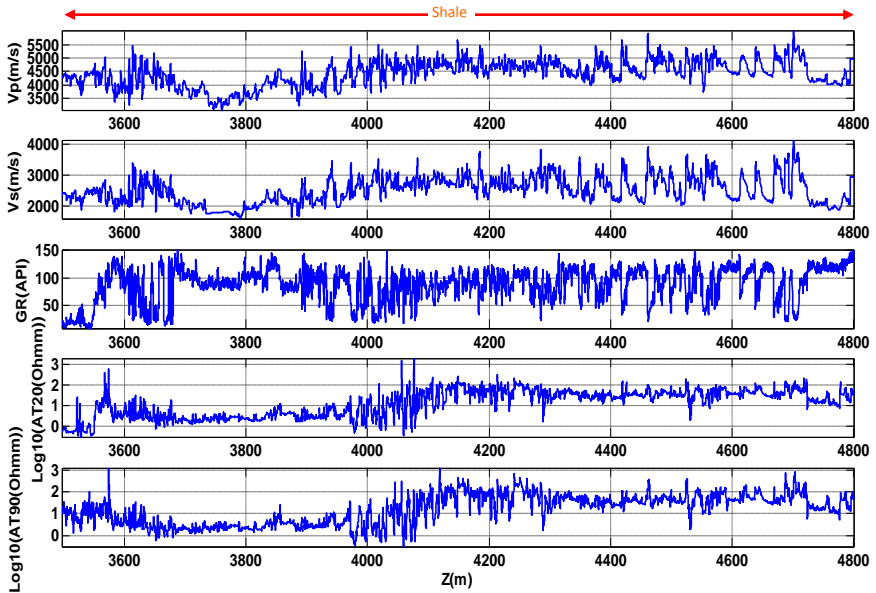


Figure 4. Physical properties measured within the depth interval (3497 -4801 m) in borehole W4. Symbols as in Table 1. Log: decimal logarithm.

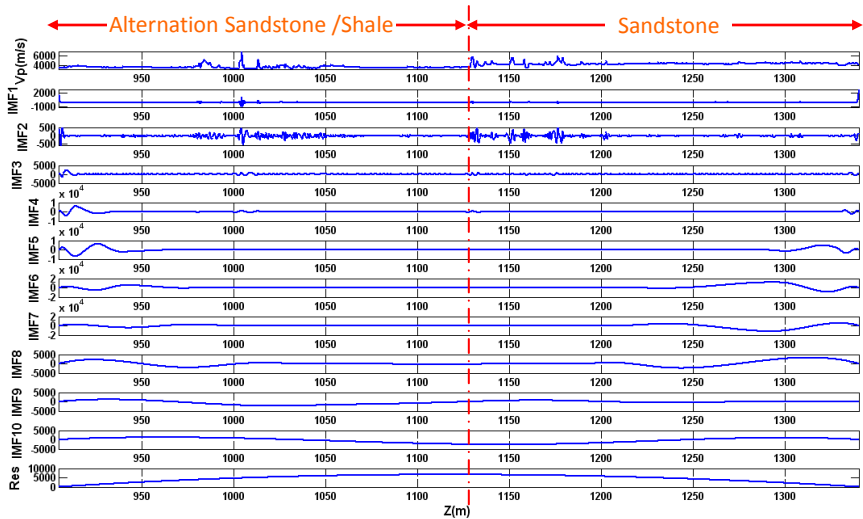


Figure 5. From top to bottom: Vp log recorded in borehole W1; 10 IMFs and residue resulting from EMD (given in m/s). The vertical red line denotes the separation between the layers composing the studied depth interval.

In this paper, only the results obtained from Vp log recorded in well W1 are presented. Figure 5 reports the 10 IMFs and residue resulting from EMD, and the boundary between the layers (Alternation Sandstone /Shale, and Sandstone), found in the studied depth interval, is marked by a red vertical line. Graphically, it can be noted that the characteristic spatial scale of fluctuations in each IMF is increasing with the mode number m , and each IMF has its specific mean wavenumber. Hence, the data are divided into locally non-overlapping depth scale components.

As regards Figure 6, it displays the power spectral densities (PSDs) of all IMFs (from 1 to 10) plotted in a log-log plan (left side) and the mean wavenumber versus the mode number m viewed in a log-linear plan (right side). The top and bottom panels correspond to the first and second lithological subintervals, respectively. For both investigated lithological units, an exponential decrease of the mean wavenumber with the mode number m is observed. This behavior power law is expressed by: $k_m = k_0 \rho^{-m}$ where $\rho=1.860 \pm 0.016$ and 1.784 ± 0.021 is determined, respectively, for the first and second lithological units. This property corresponds to an almost dyadic filter bank in the wavenumber domain.

For recall, a dyadic filter bank is a set of band-pass filters presenting a constant band-pass shape (e.g., a Gaussian distribution) but with adjacent filters covering half or double of the frequency range of any single filter in the bank. The frequency ranges of the filters can be overlapped.

The above analysis, performed on Vp log corresponding to well W1, has been extended to the other well logs, and the results obtained from wells W1, W2, W3 and W4 are summarized, respectively, in Tables 2, 3, 4, and 5. Each table gives the number of total log points N , the expected total number of IMFs $\log_2(N)$

(which is the case of white noise data), the actual total number of IMFs, the lithology of the depth subintervals and the estimated ρ value corresponding to each lithological subinterval.

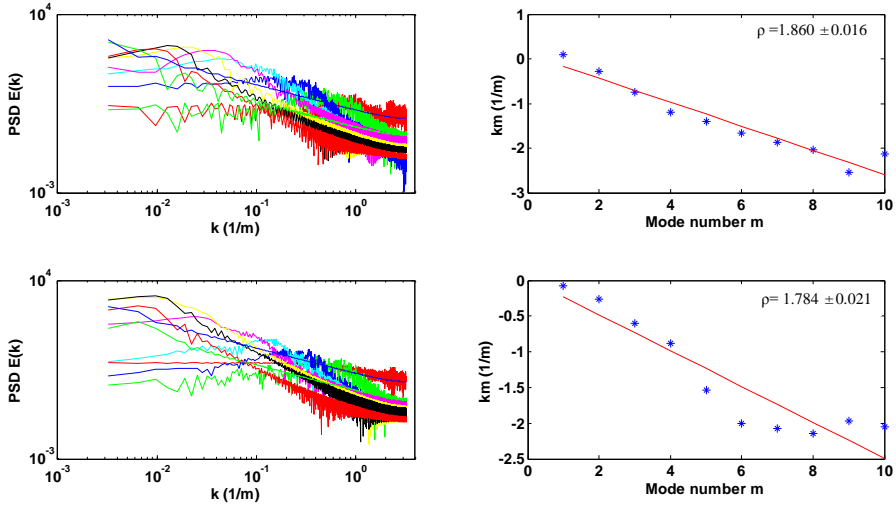


Figure 6. On the left: Power spectral densities of all IMFs (from 1 to 10) obtained from Vp log in Figure 5 using EMD method (each color corresponds to a IMF). On the right: representation of the mean wavenumber vs. mode number m in a log-linear plan. The top and the bottom panels correspond, respectively, to the two layers composing the studied depth interval: alternation Sandstone /Shale and Shale.

From Tables 2-5, it can be seen that for all the investigated logs, the total number of IMFs resulting from the EMD decomposition is less than $\log_2(N)$. This statement may be explained by the fact that the investigated logs are not purely stochastic noise and probably show intermittency properties in certain scales causing mode mixing.

Table 2. Results obtained from the application of EMD method to logs recorded in well W1.

| W1 Log (N= 2854) | IMFs number (log2(N)-11) | Lithology | ρ value |
|---------------------|--------------------------|-------------|-------------------|
| Vp | 10 | Alternation | 1.860 \pm 0.016 |
| | | Sandstone | 1.784 \pm 0.021 |
| rhob | 9 | Alternation | 2.202 \pm 0.021 |
| | | Sandstone | 2.124 \pm 0.040 |
| nphi | 9 | Alternation | 2.066 \pm 0.020 |
| | | Sandstone | 1.910 \pm 0.020 |
| GR | 9 | Alternation | 2.062 \pm 0.024 |
| | | Sandstone | 1.833 \pm 0.013 |
| PEF | 9 | Alternation | 2.029 \pm 0.017 |
| | | Sandstone | 1.878 \pm 0.023 |
| LLD | 9 | Alternation | 1.895 \pm 0.022 |
| | | Sandstone | 1.948 \pm 0.017 |
| Th | 9 | Alternation | 2.173 \pm 0.020 |
| | | Sandstone | 1.948 \pm 0.017 |
| U | 9 | Alternation | 2.083 \pm 0.015 |
| | | Sandstone | 1.974 \pm 0.020 |
| Average for well W1 | | | 1.985 \pm 0.020 |

Table 3. Results obtained from the application of EMD method to logs recorded in well W2.

| W2 Log (N=1561) | IMFs number (log2(N)-11) | Lithology | ρ value |
|---------------------|--------------------------|-----------|-------------------|
| Vp | 8 | Sandstone | 1.960 \pm 0.024 |
| | | Shale | 2.022 \pm 0.031 |
| Vs | 7 | Sandstone | 2.198 \pm 0.031 |
| | | Shale | 1.968 \pm 0.025 |
| GR | 8 | Sandstone | 1.958 \pm 0.017 |
| | | Shale | 1.907 \pm 0.028 |
| AT20 | 8 | Sandstone | 1.981 \pm 0.033 |
| | | Shale | 1.851 \pm 0.020 |
| AT90 | 8 | Sandstone | 1.691 \pm 0.028 |
| | | Shale | 1.746 \pm 0.023 |
| Average for well W2 | | | 1.928 \pm 0.026 |

Table 4. Results obtained from the application of EMD method to logs recorded in well W3.

| W3 Log (N=901) | IMFs number (log ₂ (N)~10) | Lithology | ρ value |
|---------------------|---------------------------------------|-----------|--------------|
| rhob | 7 | Sandstone | 1.873 ±0.039 |
| | | Shale | 1.735 ±0.039 |
| PEF | 7 | Sandstone | 1.808 ±0.017 |
| | | Shale | 1.801 ±0.014 |
| GR | 7 | Sandstone | 1.803 ±0.013 |
| | | Shale | 1.902 ±0.023 |
| Th | 8 | Sandstone | 1.955 ±0.015 |
| | | Shale | 2.103 ±0.020 |
| K | 7 | Sandstone | 1.857 ±0.026 |
| | | Shale | 1.924 ±0.037 |
| Average for well W3 | | | 1.876±0.024 |

Table 5. Results obtained from the application of EMD method to logs recorded in well W4.

| W4 Log (N=8558) | IMFs number (log ₂ (N)~13) | Lithology | ρ value |
|---------------------|---------------------------------------|-----------|--------------|
| Vp | 10 | Shale | 2.265 ±0.011 |
| Vs | 11 | Shale | 2.031 ±0.011 |
| GR | 11 | Shale | 2.149 ±0.012 |
| AT20 | 12 | Shale | 1.931 ±0.011 |
| AT90 | 12 | Shale | 1.853 ±0.008 |
| Average for well W4 | | | 2.046 ±0.011 |

As described in Section 2, ρ value provides a measure of multi-scale aspects of the signal and complexity of the analyzed phenomenon. Indeed, a lower value implies that more scales are considered in EMD decomposition. Hence, the studied signal displays a more complex behavior.

In this view, this parameter is estimated for all the available datasets related to the considered boreholes in order to characterize heterogeneities occurred in the studied depth ranges. Figure 7 reports the estimated ρ values corresponding to the different lithological units for all the analyzed well logs. The obtained results show that for a given well, the investigated lithological subintervals are generally

characterized by distinct ρ values, except for PEF log (well w3) where sandstone and shale layers are described by very close values. As it can be noted from Figure 8, the histogram of ρ values calculated for all the borehole logs follows a normal distribution with a mean value of 1.952 and a standard-deviation of 0.137 where ρ value varies between 1.691 ± 0.028 and 2.265 ± 0.011 . It is also noted that for a given well, logs are described by different ρ values, thus by a range of complexity levels, which depend on the lithology and the recorded physical property.

On the other hand, an average ρ value is computed for each borehole: 1.985 ± 0.020 (W1), 1.928 ± 0.026 (W2), 1.876 ± 0.024 (W3) and 2.046 ± 0.011 (W4). All these values are very close to 2 and the slight difference may be originated from intermittency. This result illustrates that the EMD acts as an almost dyadic filter bank in the wavenumber domain, as previously obtained for stochastic simulations of fGn and white noise, as well as for turbulence time series.

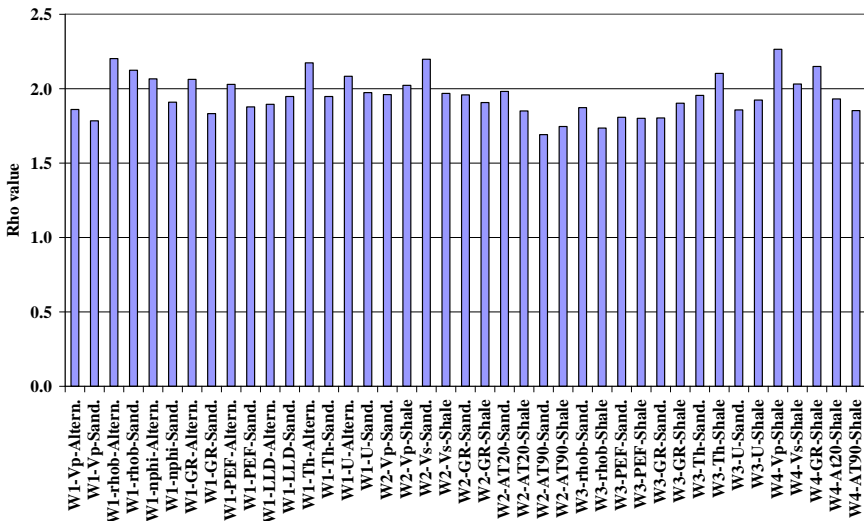


Figure 7. The ρ value estimated for all the lithological subintervals corresponding to all the analyzed well logs.

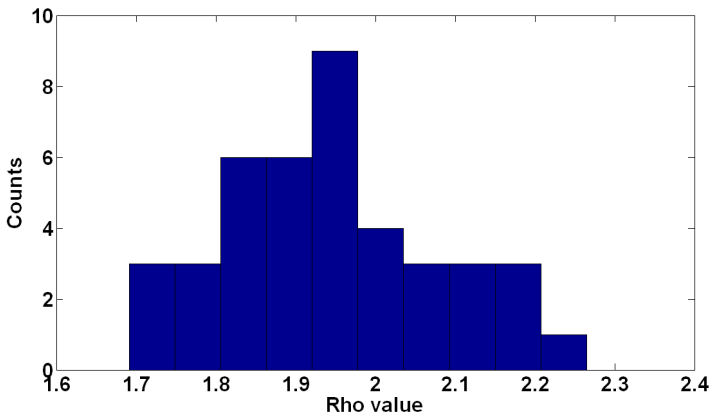


Figure 8. Histograms of the ρ value obtained from logs recorded in the considered boreholes.

Now, the next step is a lithological characterization that consists of calculating an average ρ value related to each specific lithology for each borehole taken independently, then for all the available boreholes (Table 6). It is worth mentioning that the lithology crossed by the considered boreholes is described by very close average ρ values, thus a specific lithology cannot be characterized by a ρ value. An investigation on a large number of well logs is in progress in order to establish a relation between lithology and ρ value.

Table 6. Average ρ values of each lithology crossed by the considered wells.

| Lithology | Well | Averaged ρ value |
|-------------|-----------|-----------------------|
| Alternation | W1 | 2.046 ± 0.019 |
| | W2 | 2.046 ± 0.011 |
| Sandstone | W1 | 1.925 ± 0.021 |
| | W2 | 1.958 ± 0.027 |
| | W3 | 1.859 ± 0.022 |
| | W1, 2 & 3 | 1.916 ± 0.023 |
| | W4 | 1.946 ± 0.021 |
| Shale | W2 | 1.899 ± 0.025 |
| | W3 | 1.893 ± 0.026 |
| | W4 | 2.046 ± 0.011 |
| | W2, 3 & 4 | 1.946 ± 0.021 |

7.6 Conclusion

In this paper, we analyzed the multi-scales features of physical measurements recorded in four Algerian exploration boreholes, drilled in different geological settings, using the EMD decomposition. The latter highlighted the complexity and the multi-scale nature of logs related to lithology traversed by the considered wells.

It is found that the EMD analysis behaves as an almost dyadic filter bank in wavenumber domain. Besides, using the ρ coefficient, it offers the opportunity to characterize subsurface heterogeneities: the lower ρ value, the more complex the explored geological medium. However, this technique fails to assign a specific ρ value to a given lithology. An extended investigation on a larger number of datasets, corresponding to boreholes drilled in diverse geological settings, is needed to a clear relation between this parameter, lithology and the measured physical property.

Acknowledgment

I acknowledge SONATRACH- Division Exploration for providing the data published in this paper.

References

- [1] Bekara, M., and Van der Baan, M., 2009. Random and coherent noise attenuation by empirical mode decomposition: *Geophysics*, 74 (5), V89-V98, doi: 10.1190/1.3157244.
- [2] Chiew, F., Peel, M., Amirthanathan, G., and Pegram, G.G.S., 2004. Identification of oscillations in historical global streamflow data using Empirical Decomposition, Seventh IAHS Scientific Assembly-Symposium on Regional Hydrological Impacts of Climate Variability and Change with an Emphasis on Less Developed Countries.

- [3] De Michelis, P., Consolini, G., and Tozzi, R., 2012. On the multi-scale nature of large geomagnetic storms: an empirical mode decomposition analysis, *Nonlin. Processes Geophys.*, 19, 667-673.
- [4] Flandrin, P. and Gonçalves, P., 2004. Empirical mode decompositions as data driven wavelet-like expansions, *Int. J. Wavelets, Multires. Info. Proc.*, 2, 477-496.
- [5] Flandrin, P., Rilling, G., and Gonçalves, P., 2004. Empirical mode decomposition as a filter bank, *IEEE Sig. Proc. Lett.*, 11, 112-114.
- [6] Han, J., and Van der Baan, M., 2011. Empirical mode decomposition and robust seismic attribute analysis: CSPG CSEG CWLS Convention, 114.
- [7] Gloerson, P. and Huang, N. E., 2003. Comparison of interannual intrinsic modes in hemispheric sea ice covers and others geophysical parameters, *IEEE Transactions on Geoscience and Remote Sensing*, 41 (5), 1062-1074.
- [8] Huang, N. E., Shen, Z., Long, S. R., Wu, M. C., Shih, E. H., Zheng, Q., Tung, C. C. and Liu, H. H., 1998. The empirical mode decomposition method and the Hilbert spectrum for non-stationary time series analysis, *Proc. Roy. Soc. London* 454A, 903-995.
- [9] Huang, N. E., Shen, Z. and Long, R. S., 1999. A new view of nonlinear water waves — the Hilbert spectrum, *Ann. Rev. Fluid Mech.* 31, 417-457.
- [10] Huang, N. E., Wu, M. L., Long, S. R., Shen, S. S. P., Qu, W., Gloersen, P., Fan, K. L., 2003. A confidence limit for the empirical mode decomposition and Hilbert spectral analysis, *Proc. R. Soc. London, Ser. A* 459 (2037), 2317-2345.
- [11] Huang, N. E., 2005. Hilbert-Huang Transform and Its Applications. World Scientific, Ch. 1. Introduction to the hilbert huang tranform and its related mathematical problems, pp. 1-26.
- [12] Huang, N. E. and Wu, Z., 2008. A review on Hilbert-Huang Transform: Methods and its applications to geophysical studies, *Rev. Geophys.*, 46, RG2006, doi: 10.1029/2007RG000228.
- [13] Huang, Y., Schmitt, F., Lu, Z., Liu, Y., 2008. An amplitude-frequency study of turbulent scaling intermittency using hilbert spectral analysis, *Europhys. Lett.* 84 40010.

- [14] Rilling, G., Flandrin, P., Gonçalvès, P., 2003. On empirical mode decomposition and its algorithms. IEEE-EURASIP Workshop on Nonlinear Signal and Image Processing.
- [15] Rilling, G., Flandrin, P., 2008. One or two frequencies? The empirical mode decomposition answers, IEEE Trans. Signal Process, 85-95.
- [16] Wu, Z. and Huang, N. E., 2004. A study of the characteristics of white noise using the empirical mode decomposition method, P. Roy. Soc. A-Math. Phy., 460, 1597-1611.